Inorganic Chemistry

Article

pubs.acs.org/IC

Two Nanocage-Based Metal–Organic Frameworks with Mixed-Cluster SBUs and CO_2 Sorption Selectivity

Bo Liu,[†] Wei-Ping Wu,[†,‡] Lei Hou,[†] Zhi-Sen Li,[†] and Yao-Yu Wang*[,†]

[†]Key Laboratory of Synthetic and Natural Functional Molecule Chemistry of the Ministry of Education, Shaanxi Key Laboratory of Physico-Inorganic Chemistry, College of Chemistry & Materials Science, Northwest University, Xi'an 710069, P. R. China

[‡]Institute of Functional Materials, College of Chemistry and Pharmaceutical Engineering, Sichuan University of Science & Engineering, Zigong 643000, P. R. China

Supporting Information

ABSTRACT: Two nanocage-based metal–organic frameworks respectively built on two and three types of clusters with diisophthalate ligand were constructed, displaying unprecedented (3,4,6)-connected nets, unusual nanocages, and new bipaddle-wheel tetranuclear cluster, as well as highly selective CO_2 capture.

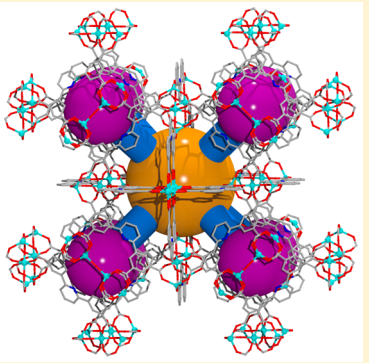

INTRODUCTION

Metal–organic frameworks (MOFs), as one of the most rapidly developing fields in chemical and material sciences, are emerging as an important family of porous materials because of their intriguing topologies and exploitable properties.[1] Metal–organic polyhedral cages and cage-based MOFs with special internal voids possess a broad spectrum of potential uses as materials. The cage-type assembly can serve as a trap to selectively capture a particular guest molecule based on its chemical and physical properties,[2] and the most impressive is a very promising material for CO_2 capture and separation.[3] A large number of examples have proven that the combination of angular organic linkers with inorganic secondary building units (SBUs) is the most important and practical strategy to build cages.[4] In this regard, the various metal–organic clusters as SBUs have been created for cage fabricating.[5] Notably, in those reports, major cages were constructed by the single inorganic SBUs, whereas the cages based on binary, ternary, or more inorganic SBUs are unique with multivariate functionalities and heterogeneous pores in ordered assemblies,[6] which were observed only in sporadic complexes.[7] Therefore, the design and synthesis of novel cage-based MOFs based on mixed-cluster SBUs would be of great significance and an appealing challenge.

The recent advances show that the isophthalate units by combining inorganic clusters are very useful to form discrete cages, and the elongated isophthalate linkers connect adjacent cages to generate high dimensional cage-based MOFs.[8] The 2,6-di(3′,5′-dicarboxylphenyl)pyridine (H_4L) is a much less-investigated ligand, which contains two separated isophthalate subunits with the included angle of ∼120° and central pyridyl spacer. Moreover, the electron conjugated effect of the central pyridine in H_4L makes the whole ligand molecule lie in the same plane, which is conducive to form the high-symmetry frameworks. Our recent report confirmed that the unique configuration of four carboxylate groups in H_4L make it very favorable to link lanthanide ion clusters to generate nanocage-based MOFs.[9] Inspired by the Ln-nanocage MOFs results, how about the transition metal ions? Generally, the transition metal ions due to low coordination numbers prefer forming multinuclear clusters, especially for Zn^{2+} and Mn^{2+}; their versatile cluster-based MOFs were frequently observed.[10] As we expected, herein, by reacting H_4L with $Zn(NO_3)_2$ or $MnCl_2$ under solvothermal conditions, two new MOFs with high-symmetry (3,4,6)-connected nets, namely, $[Zn_2(L)(H_2O)_{1.5}]\cdot 5H_2O$ (**1**) and $[H_2N(CH_3)_2]_5[Mn_{13}(L)_6(Cl)_3(HCOO)_4(DMF)_4(H_2O)_{2.7}]\cdot 2DMF\cdot 4H_2O$ (**2**; DMF = dimethylformamide), were successfully constructed, revealing unusual nanocage-based frameworks with very rare two or three types of cluster SBUs, which include an interesting bipaddle-wheel tetranuclear cluster.

EXPERIMENTAL SECTION

Materials and Measurements. All reagents and solvents were commercially available and were used without further purification. Infrared spectra were obtained in KBr discs on a Nicolet Avatar 360 FTIR spectrometer in the 400–4000 cm^{-1} region. Elemental analyses (C, H, and N) were performed with a PerkinElmer 2400C Elemental Analyzer. Thermalgravimetric analyses (TGA) were performed in

Received: May 5, 2015
Published: September 10, 2015

DOI: 10.1021/acs.inorgchem.5b00987
Inorg. Chem. 2015, 54, 8937–8942

nitrogen stream using a Netzsch TG209F3 equipment at a heating rate of 5 °C/min. Powder X-ray diffraction (PXRD) data were recorded on a Bruker D8 ADVANCE X-ray powder diffractometer (Cu Kα, 1.5418 Å). All the gas sorption isotherms were measured by using an ASAP 2020 M adsorption equipment. The activated samples of **1** were prepared by direct heating the as-synthesized samples in a quartz tube under high vacuum at 170 °C for 2.5 h and then heating at 190 °C for 2 h to remove the solvated and coordinated water molecules prior to measurements. Similarly, the guest molecules and coordinated DMF molecules in **2** can be removed by direct heat of **2** at 130 °C in a quartz tube under high vacuum for 3 h and subsequent heating at 150 °C for 2 h for gas adsorption measurements.

Synthesis of $[Zn_2(L)(H_2O)_{1.5}]\cdot 5H_2O$ (1). A mixture of H_4L (12.22 mg, 0.03 mmol) and $Zn(NO_3)_2\cdot 6H_2O$ (17.85 mg, 0.06 mmol) was dissolved in dimethylacetamide (DMA)/EtOH/CH_3CN (1:1:1, 4.5 mL) in a screw-capped vial. After two drops of HNO_3 (63%, aq.) and 0.1 mL of H_2O were added to the mixture, the vial was capped and placed in an oven at 105 °C for 72 h. The resulting single crystals were washed with DMA several times to give **1**. The yield was ~15 mg (~74% based on H_4L). Anal. (%) Calcd for $[Zn_2(L)(H_2O)_{1.5}]\cdot 5H_2O$: C, 38.73; H, 3.40; N, 2.15; found: C, 38.61; H, 3.59; N, 2.33. (IR (KBr, cm^{-1}): 3409(m), 2933(m), 2363(m), 1882(w), 1613(s), 1580(m), 1440(m), 1400(s), 1310(w), 1272(m), 1180(m), 1107(m), 1020(m), 925(m), 776(s), 721(s), 656(m), 597(w), 478(m).

Synthesis of $[H_2N(CH_3)_2]_5[Mn_{13}(L)_6(Cl)_3(HCOO)_4(DMF)_4(H_2O)_{2.7}]\cdot 2DMF\cdot 4H_2O$ (2). A mixture of H_4L (12.22 mg, 0.03 mmol) and $MnCl_2\cdot 4H_2O$ (11.87 mg, 0.06 mmol) was dissolved in DMF (4 mL) in a screw-capped vial. After four drops of HNO_3 (63%, aq.) and 0.1 mL of H_2O were added to the mixture, the vial was capped and placed in an oven at 90 °C for 60 h. The resulting single crystals were washed with DMF several times to give **2**. The yield was ~14 mg (~62% based on H_4L). Anal. (%) Calcd for $[H_2N(CH_3)_2]_5[Mn_{13}(L)_6(Cl)_3(HCOO)_4(DMF)_4(H_2O)_{2.7}]\cdot 2DMF\cdot 4H_2O$: C, 44.71; H, 2.86; N, 4.23; found: C, 44.79; H, 2.64; N, 4.40. (IR (KBr, cm^{-1}): 3412(m), 3080(w), 2959(w), 2926(m), 2800(m), 2465(m), 1970(w), 1878(m), 1660(s), 1639(s), 1612(m), 1571(s), 1438(m), 1392(s), 1358(s), 1272(m), 1179(s), 1102(s), 1020(m), 923(m), 865(w), 778(s), 716(s), 655(s), 461(m).

Crystallography. The diffraction data were collected at 296(2) K for **1** and **2**, respectively, with a Bruker-AXS SMART CCD area detector diffractometer using ω rotation scans with a scan width of 0.3° and Mo Kα radiation (λ = 0.710 73 Å). Absorption corrections were performed utilizing SADABS routine.[11] The structures were solved by direct methods and refined using the SHELXTL 97 software.[12] Atoms were located from iterative examination of difference F-maps following least-squares refinements of the earlier models. All the atoms except hydrogen atoms, which were fixed at calculated positions and refined by using a riding mode, were refined anisotropically until full convergence was achieved. The large voids in the structure **1** allow for considerable flexing and uncertainty in the positions of the framework atoms, and this is evidenced in large atomic displacement parameters for many of the pyridine carbons and nitrogens from ligand. It was necessary to constrain or restrain a number of bond lengths in the structure to get a stable refinement and chemically reasonable model. All carbon and nitrogen atoms from pyridines in **1** were restrained to have similar atomic displacement parameters as their neighbors in the refinement. Because of the large cages in **1** and **2**, the guest solvents in the crystals are highly disordered and impossible to refine using conventional discrete-atom models; the SQUEEZE[13] subroutine of the PLATON software suite was applied to remove the scattering from the highly disordered solvent molecules. Crystal data as well as details of data collection and refinements for both **1** and **2** are summarized in Table 1.

Table 1. Crystal Data and Structure Refinements for 1 and 2

complex	**1**	**2**
empirical formula	$C_{21}H_{12}NO_{9.5}Zn_2$	$C_{142}H_{91}Cl_3Mn_{13}N_{10}O_{62.5}$
formula mass	561.08	3757.82
temperature [K]	296(2)	296(2)
crystal system	cubic	tetragonal
space group	$Im\bar{3}$	$I4/m$
a [Å]	27.468(3)	26.318(8)
b [Å]	27.468(3)	26.318(8)
c [Å]	27.468(3)	30.474(9)
α [deg]	90.00	90.00
β [deg]	90.00	90.00
γ [deg]	90.00	90.00
V [Å^3]	20 724(2)	21 107(11)
Z	24	4
D_{calcd}.[g·cm^{-3}]	1.071	1.183
μ [mm^{-1}]	1.424	0.857
GOF on F^2	1.091	1.137
reflns collected/unique	54 436/1951	56 622/10 570
R_{int}	0.0566	0.0332
R_1,[a] wR_2 [b] [$I > 2\sigma(I)$]	0.0961, 0.2155	0.0687, 0.2077
R_1, wR_2 (all data)	0.1029, 0.2189	0.0783, 0.2177

[a] $R_1 = \sum||F_o| - |F_c||/\sum|F_o|$. [b] $wR_2 = [\sum w(F_o^2 - F_c^2)^2/\sum w(F_o^2)^2]^{1/2}$.

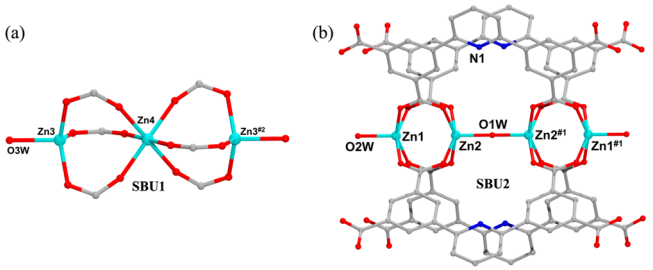

Figure 1. Structures of SBU1 (a) and SBU2 (b) in **1**, symmetry codes: No. 1 2 − x, 2 − y, 1 − z; No. 2 1.5 − x, 1.5 − y, 0.5 − z.

RESULTS AND DISCUSSION

Crystal Structure. Complex **1** crystallizes in cubic system $Im\bar{3}m$ space group with four independent Zn^{2+} ions, one L^{4-}, and 1.5 water ligands in the asymmetric unit. As shown in Figure 1, **1** contains two different clusters as SBUs: one is the classical linear trinuclear Zn_3 cluster (S_6 symmetry, SBU1) with a C_3 axis threading three Zn^{2+} ions (Figure 1a), in which the outer Zn^{2+} ion adopts tetrahedral coordination with three carboxylate O atoms and one water molecule, while the central Zn^{2+} ion is octahedrally coordinated by six symmetry-related O atoms from six carboxylate groups; the other is a tetranuclear Zn_4 cluster (SBU2) with a C_4 axis threading four Zn^{2+} ions (Figure 1b), which is a very novel bipaddle-wheel SBU formed by a central μ_2-H_2O molecule bridging two $Zn_2(COO)_4$ paddle-wheel subunits. Although $M_2(COO)_4$ SBU has been intensively investigated, the bipaddle-wheel SBU is previously never observed in complexes. The generation of bipaddle-wheel SBU in **1** is attributed to the unique geometry of two closest carboxylate groups between −Ph−Py−Ph− spacer, which shows planarity and has a 3.75 Å separation, so one water molecule can insert into the middle of two $Zn_2(COO)_4$ subunits.

Interestingly, two nanocages based on the mixed-cluster SBUs are formed in **1**. Two SBU2 and four SBU1 form an octahedral M_6L_4 nanocage (**Cage I**, Figure 2a) with an inner diameter of ~1.4 nm, and four L^{4-} linkers as faces, as well as four triangle windows of sizes ca. 4.3 × 5.0 × 5.6 Å^3 (excluding van der Waals radii of the atoms). The adjacent **Cage I** are joined together by coshared SBU2 along the cell axes. The most striking structural feature is that a bigger $M_{14}L_{32}$ nanocage (**Cage II**, Figure 2b) of inner diameter ~1.8 nm is formed by eight SBU1, six SBU2, and thirty-two L^{4-} linkers. This charming **Cage II** contains 48

DOI: 10.1021/acs.inorgchem.5b00987
Inorg. Chem. 2015, 54, 8937−8942

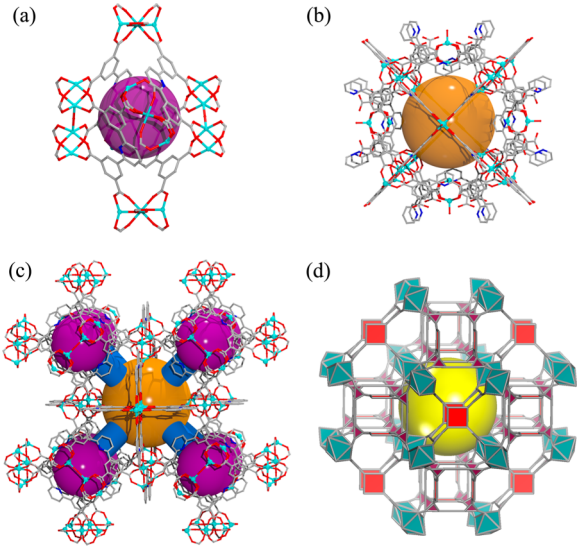

Figure 2. Structures of M_6L_4 **Cage I** (a) and $M_{14}L_{32}$ **Cage II** (b) in **1**, the 3D structure (c) of **1** and its topology (d), forming 3D porous system (only eight **Cage I** around one **Cage II** are drawn for clarity).

vertices, as we know, which represents the highest vertical number in present cage-based coordination systems.[2−5,7] Meanwhile, the **Cage II** contains 24 six-memerbed faces as windows with face symbol 6^{24} which also first appears in complexes.

The adjacent **Cage I** and **Cage II** in **1** are united by corner and edge sharings to afford a three-dimensional (3D) open framework (Figure 2c). The framework possesses a 3D porous system with the cosharings of triangle windows of cages in which each **Cage II** connects 24 **Cage I** by 24 windows, while each **Cage I** joins four **Cage II** by four windows. The accessible solvent void is 51.7% after the removal of terminal aqua ligands and free guest molecules. Topologically, considering the H_4L linker is a branched tetratopic linker, each L^{4-} can be treated as two linked 3-c nodes, meanwhile leaving the bipaddle-wheel (SBU2) as two 4-c nodes and SBU1 as six-connected nodes, so the framework can be designated as a trinodal (3,4,6)-connected net with the new topology of point symbol $(6{\cdot}7^2)_{12}(6^6)_3(7^6{\cdot}8^6{\cdot}11^3)_2$ (Figure 2d and Figure S4 in the Supporting Information).[14] Among the numerous topological nets, the (3,4,6)-connected nets are extremely scarce because they require three different numbers of nodes, and even only 13 examples were enumerated in RCSR database.[15] Importantly, comparing to those topologies, such a topology in **1** is indeed rare due to its highest symmetry, and to our best knowledge it is herein first observed in complexes.

Complex **2** crystallizes in the tetragonal space group $I4/m$ with seven independent Mn^{2+} ions, two L^{4-}, two chloride anions, and one formate ligand in the asymmetric unit. The Mn^{2+} ions show tetragonally pyramidal and octahedral coordination geometries. Two L^{4-} are almost planar, possessing the similar coordination modes (Figure S1 in the Supporting Information). Interestingly, **2** contains three different clusters as SBUs: SBU3 and SBU4 are tetranuclear bipaddle-wheel clusters (Figure 3a,b), which are similar to SBU2 in **1**; besides, the two axial aqua ligands in SBU2 are replaced by chlorine atoms, acting as terminal and μ_2-bridging ligands in SBU3 and SBU4, respectively. SBU5 is a linear trinuclear cluster (Figure 3c), resembling SBU1 in **1**; however, the difference is that each SBU5 in **2** is further connected two Mn7 atoms by two outer formate ligands. Thus, each Mn7 atom connects four SBU5 and one SBU4 by four C_4-symmetry formate ligands and one μ_2-Cl atom (Figure 3b). Although different SBUs in **1** and **2**, **2** reveals the same 3D (3,4,6)-connected topological framework with **1**, in which SBU3 and SBU4 serve as the same two 4-c nodes, and L^{4-} and SBU5 are simplified as two linked 3- and 6-connected nodes, respectively (Figure 4d). In **2**, two

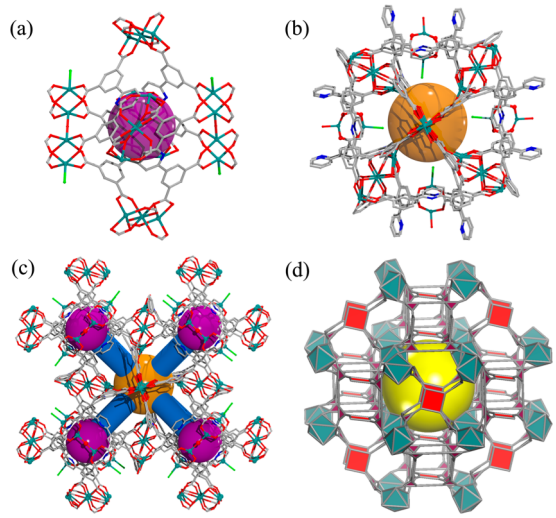

Figure 4. Structures of M_6L_4 **Cage I** (a) and $M_{14}L_{32}$ **Cage II** (b) in **2**, the 3D structure (c) of **2** and its topology (d), forming 3D porous system (only eight **Cage I** around one **Cage II** are drawn for clarity).

SBU3, four SBU5, and four N1-containing L^{4-} form an octahedral M_6L_4 nanocage with inner diameter of ~1.2 nm and triangle windows of sizes ca. 3.5 × 3.7 × 4.5 Å^3. Two SBU4, four SBU3, eight SBU5, and 12 N1-containing and 12 N2-containing L^{4-} form a bigger $M_{14}L_{32}$ nanocage ($d \approx 1.3$ nm), resembling the situations in **1** (Figure 4a,b). The adjacent cages are intersected

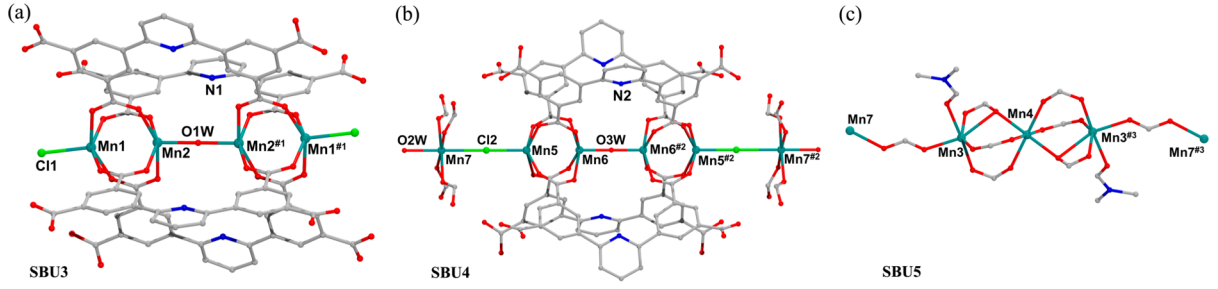

Figure 3. Structures of SBU3 (a), SBU4 (b), and SBU5 (c) in **2**, symmetry codes: No. 1 2 − x, 1 − y, 2 − z; No. 2 1 − x, 1 − y, 1 − z; No. 3 1.5 − x, 0.5 − y, 1.5 − z.

DOI: 10.1021/acs.inorgchem.5b00987
Inorg. Chem. 2015, 54, 8937−8942

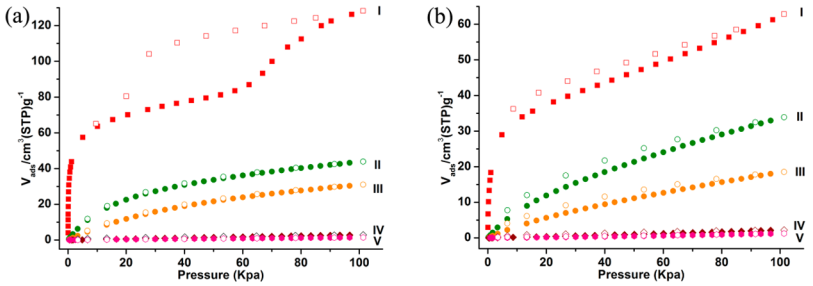

Figure 5. Sorption isotherms of **1** (a) and **2** (b): CO_2 195 K (I), 273 K (II), 298 K (III), CH_4 298 K (IV), and N_2 298 K (V).

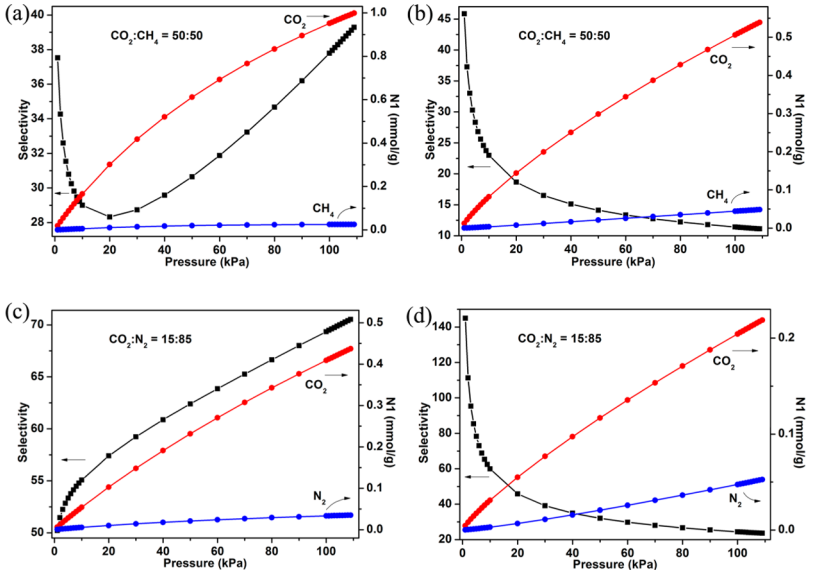

Figure 6. IAST adsorption selectivities and isotherms of **1** and **2** for equimolar mixtures of CO_2 and CH_4 (a, b) and a mixture of CO_2 (15%) and N_2 (85%) (c, d) at 298 K.

to yield a 3D open framework with a 3D porous system (Figure 4c); the free void is 48.3% after excluding terminal ligands, $Me_2(NH_2)^+$ cations, and solvent molecules.

Complexes **1** and **2** are two and three mixed-cluster SBUs-based frameworks, respectively. The mixing of multiple inorganic cluster SBUs represents a typical but less explored approach to achieve heterogeneity within order, in particular, in MOF materials.[6] Despite that a large number of cluster-based MOFs have been found, the mixed-clusters-based MOFs are extremely rare in complexes.[16]

Sorption Properties. To estimate the porosity of **1** and **2**, N_2, CO_2, and CH_4 gas adsorption measurements were performed. As shown in Figures 5, S9, and S10 (Supporting Information), the activated **1** and **2** show approximate adsorption isotherms and significant uptakes for CO_2 at both low and enhanced temperatures, but almost exclude N_2 and CH_4. At 195 K and 1 atm, the CO_2 uptakes for **1** and **2** are 128.3 (5.73 mmol g^{-1}) and 62.9 (2.81 mmol g^{-1}) cm^3 g^{-1}, respectively, which are much higher than CH_4 uptakes (19.8 cm^3 g^{-1} for **1** and 14.9 cm^3 g^{-1} for **2**). The Langmuir (BET) surface areas calculated from the first step adsorption isotherms are 347(240) and 194(132) m^2 g^{-1} for **1** and **2**, respectively, within the pressure range of $0.05 < P/P_0 < 0.3$.[17] The higher CO_2 loadings of **1** relative to **2** should be attributed to the larger effective free void of **1**. At low temperature, the stepwise isotherm of CO_2 (195 K) for **1** and N_2 (77 K) for **2** should be attributed to the nanosized intercrystalline voids or mesopores within the mosaic pseudomorphs that remain after desolvation.[18] At higher temperatures of 273 and 298 K, the selective tendencies for CO_2 in **1** and **2** are more obvious. For **1**, the adsorption amounts of CO_2 at 273 and 298 K are 43.9 and 31.0 cm^3 g^{-1}, respectively, but only a trace of CH_4 (2.9 cm^3 g^{-1}) and N_2 (1.4 cm^3 g^{-1}) uptakes at 298 K. For **2**, the CO_2 uptakes are 33.9 and 18.5 cm^3 g^{-1}, while the CH_4 and N_2 uptakes are 2.2 and 1.2 cm^3 g^{-1} at 273 and 298 K, respectively. The CO_2 adsorption enthalpies are ca. 28.6−24.9 kJ mol^{-1} for **1** and 28.8−21.5 kJ mol^{-1} for **2** in the whole CO_2 coverage region (Figure S12 in the Supporting Information). The intermediate adsorption enthalpies for **1** and **2** imply the low-energy consumption for adsorbent regeneration, a desired property for separation applications.[19]

The selectivities of **1** and **2** for CO_2/CH_4 and CO_2/N_2 in gas mixtures were further characterized at 298 K by the ideal adsorbed solution theory[20] (IAST; Figure S13 in the Supporting Information). The predicted adsorption selectivities of CO_2/CH_4 with mole ratios of 50:50 as a function of total bulk pressure are shown in Figure 6. Both **1** and **2** exhibit high initial CO_2/CH_4 selectivities (38 for **1** and 46 for **2**); even at **1** atm, the selectivities of **1** and **2** are 39 and 11, respectively, among the highest reported values for MOFs,[21] comparing with the single-molecule traps (SMTs).[3a] For the mixtures composed of 15% CO_2 and 85% N_2, a typical flue gas composition in postcombustion process, the selectivities are in the ranges of 50−71 for **1** and 24−145 for **2**. The CO_2/N_2 adsorption selectivities are comparable with those of SNU-100′ (26.5),[22] $H_3[(Cu_4Cl)_3(BTTri)_8]$ (21.0),[23] and $Cu_{24}(TPBTM)_8$ (22).[24] The significant selectivities of CO_2 over CH_4 and N_2 imply the potential applications of

DOI: 10.1021/acs.inorgchem.5b00987
Inorg. Chem. 2015, 54, 8937−8942

1 and **2** in CO_2 capture from neutral gas or postcombustion flue gas. These results also demonstrate that the advantage of designing a cage-type assembly to specifically capture CO_2 based on its polarity and the relatively narrow windows of cages.

CONCLUSIONS

In summary, by combining a planar diisophthalate linker with unusual mixed-cluster SBUs, two novel MOFs with unique nanoscale cages have been constructed. Both of them reveal highly selective CO_2 capture. This work not only could provide a facile route to design and synthesize novel cage-based MOFs as promising functional materials but also could enrich the coordination frameworks with cages and multinuclear cluster SBUs.

ASSOCIATED CONTENT

Supporting Information

The Supporting Information is available free of charge on the ACS Publications website at DOI: 10.1021/acs.inorgchem.5b00987.

Calculation of sorption heat, IAST adsorption selectivity calculation, TGA plots, IR spectra, PXRD and sorption patterns, and illustrated molecular structures. (PDF)

X-ray crystallographic information for CCDC 1045864. (CIF)

X-ray crystallographic information for CCDC 1045906. (CIF)

AUTHOR INFORMATION

Corresponding Author

*E-mail: wyaoyu@nwu.edu.cn.

Notes

The authors declare no competing financial interest.

ACKNOWLEDGMENTS

This work is supported by NSFC (21471124, 21371142, and 21001088), NSF of Shannxi province (2013KJXX-26, 13JS114, and 2014JQ2049), and Open Foundation of Key Laboratory of Synthetic and Natural Functional Molecule Chemistry of Ministry of Education (338080060).

REFERENCES

(1) (a) Sumida, K.; Rogow, D. L.; Mason, J. A.; McDonald, T. M.; Bloch, E. D.; Herm, Z. R.; Bae, T.-H.; Long, J. R. *Chem. Rev.* **2012**, *112*, 724−781. (b) Zhang, Z.; Yao, Z.-Z.; Xiang, S.; Chen, B. *Energy Environ. Sci.* **2014**, *7*, 2868−2899. (c) Furukawa, H.; Cordova, K. E.; O'Keeffe, M.; Yaghi, O. M. *Science* **2013**, *341*, 1230444. (d) Farha, O. K.; Hupp, J. T. *Acc. Chem. Res.* **2010**, *43*, 1166−1175. (e) Li, J.-R.; Kuppler, R. J.; Zhou, H.-C. *Chem. Soc. Rev.* **2009**, *38*, 1477−1504.

(2) (a) Tranchemontagne, D. J.; Ni, Z.; O'Keeffe, M.; Yaghi, O. M. *Angew. Chem., Int. Ed.* **2008**, *47*, 5136−5147. (b) Ahmad, N.; Chughtai, A. H.; Younus, H. A.; Verpoort, F. *Coord. Chem. Rev.* **2014**, *280*, 1−27. (c) Morabito, J. V.; Chou, L.-Y.; Li, Z.; Manna, C. M.; Petroff, C. A.; Kyada, R. J.; Palomba, J. M.; Byers, J. A.; Tsung, C.-K. *J. Am. Chem. Soc.* **2014**, *136*, 12540−12543. (d) Cui, P.; Ma, Y.-G.; Li, H.-H.; Zhao, B.; Li, J.-R.; Cheng, P.; Balbuena, P. B.; Zhou, H.-C. *J. Am. Chem. Soc.* **2012**, *134*, 18892−18895.

(3) (a) Li, J.-R.; Yu, J.; Lu, W.; Sun, L.-B.; Sculley, J.; Balbuena, P. B.; Zhou, H.-C. *Nat. Commun.* **2013**, *4*, 1538. (b) Li, J.-R.; Zhou, H.-C. *Nat. Chem.* **2010**, *2*, 893−898. (c) Zheng, S.-T.; Bu, J. T.; Li, Y.; Wu, T.; Zuo, F.; Feng, P.; Bu, X. *J. Am. Chem. Soc.* **2010**, *132*, 17062−17064. (d) Huang, Y.-L.; Gong, Y.-N.; Jiang, L.; Lu, T.-B. *Chem. Commun.* **2013**, *49*, 1753−1755.

(4) (a) Tranchemontagne, D. J.; Mendoza-Cortés, J. L.; O'Keeffe, M.; Yaghi, O. M. *Chem. Soc. Rev.* **2009**, *38*, 1257−1283. (b) Perry, J. J., IV; Perman, J. A.; Zaworotko, M. J. *Chem. Soc. Rev.* **2009**, *38*, 1400−1417. (c) Guillerm, V.; Kim, D.; Eubank, J. F.; Luebke, R.; Liu, X.; Adil, K.; Lah, M. S.; Eddaoudi, M. *Chem. Soc. Rev.* **2014**, *43*, 6141−6172. (d) Chen, L.; Chen, Q.; Wu, M.; Jiang, F.; Hong, M. *Acc. Chem. Res.* **2015**, *48*, 201−210.

(5) (a) Eddaoudi, M.; Kim, J.; Wachter, J. B.; Chae, H. K.; O'Keeffe, M.; Yaghi, O. M. *J. Am. Chem. Soc.* **2001**, *123*, 4368−4369. (b) Férey, G.; Mellot-Draznieks, C.; Serre, C.; Millange, F.; Dutour, J.; Surblé, S.; Margiolaki, I. *Science* **2005**, *309*, 2040−2042. (c) Koh, K.; Wong-Foy, A. G.; Matzger, A. J. *J. Am. Chem. Soc.* **2009**, *131*, 4184−4185. (d) Li, J.-R.; Zhou, H.-C. *Angew. Chem., Int. Ed.* **2009**, *48*, 8465−8468. (e) Kang, Y.; Wang, F.; Zhang, J.; Bu, X. *J. Am. Chem. Soc.* **2012**, *134*, 17881−17884. (f) Yun, R.; Lu, Z.; Pan, Y.; You, X.; Bai, J. *Angew. Chem., Int. Ed.* **2013**, *52*, 11282−11285.

(6) Furukawa, H.; Müller, U.; Yaghi, O. M. *Angew. Chem., Int. Ed.* **2015**, *54*, 3417−3430.

(7) Nouar, F.; Eubank, J. F.; Bousquet, T.; Wojtas, L.; Zaworotko, M. J.; Eddaoudi, M. *J. Am. Chem. Soc.* **2008**, *130*, 1833−1835.

(8) (a) He, Y.; Li, B.; O'Keeffe, M.; Chen, B. *Chem. Soc. Rev.* **2014**, *43*, 5618−5656. (b) Yan, Y.; Yang, S.; Blake, A. J.; Schröder, M. *Acc. Chem. Res.* **2014**, *47*, 296−307.

(9) Liu, B.; Wu, W.-P.; Hou, L.; Wang, Y.-Y. *Chem. Commun.* **2014**, *50*, 8731−8734.

(10) (a) Zhang, W.-X.; Liao, P.-Q.; Lin, R.-B.; Wei, Y.-S.; Zeng, M.-H.; Chen, X.-M. *Coord. Chem. Rev.* **2015**, *293*−*294*, 263−278. (b) Gao, W.-Y.; Cai, R.; Meng, L.; Wojtas, L.; Zhou, W.; Yildirim, T.; Shi, X.; Ma, S. *Chem. Commun.* **2013**, *49*, 10516−10518.

(11) Bruker. *SADABS, SMART, and SAINT;* Bruker AXS Inc: Madison, WI, 2002.

(12) Sheldrick, G. M. *SHELXL-97,* program for the refinement of the crystal structures; University of Göttingen: Germany, 1997.

(13) Spek, A. L. *J. Appl. Crystallogr.* **2003**, *36*, 7−13.

(14) (a) Li, M.; Li, D.; O'Keeffe, M.; Yaghi, O. M. *Chem. Rev.* **2014**, *114*, 1343−1370. (b) O'Keeffe, M.; Yaghi, O. M. *Chem. Rev.* **2012**, *112*, 675−702.

(15) Please see the Web site of the O'Keeffe group at Arizona State University, http://rcsr.anu.edu.au.

(16) (a) Wang, Z.; Kravtsov, V. C.; Zaworotko, M. J. *Angew. Chem., Int. Ed.* **2005**, *44*, 2877−2880. (b) Wong-Foy, A. G.; Lebel, O.; Matzger, A. J. *J. Am. Chem. Soc.* **2007**, *129*, 15740−15741. (c) Schoedel, A.; Cairns, A. J.; Belmabkhout, Y.; Wojtas, L.; Mohamed, M.; Zhang, Z.; Proserpio, D. M.; Eddaoudi, M.; Zaworotko, M. J. *Angew. Chem., Int. Ed.* **2013**, *52*, 2902−2905. (d) Wang, D.; Zhao, T.; Cao, Y.; Yao, S.; Li, G.; Huo, Q.; Liu, Y. *Chem. Commun.* **2014**, *50*, 8648−8650. (e) Hu, J.-S.; Zhang, L.; Qin, L.; Zheng, H.-G.; Zhang, X.-B. *Chem. Commun.* **2015**, *51*, 2899−2902.

(17) Xiang, S.-C.; Zhang, Z.; Zhao, C.-G.; Hong, K.; Zhao, X.; Ding, D.-R.; Xie, M.-H.; Wu, C.-D.; Das, M. C.; Gill, R.; Thomas, K. M.; Chen, B. *Nat. Commun.* **2011**, *2*, 204.

(18) Moon, H. R.; Kobayashi, N.; Suh, M. P. *Inorg. Chem.* **2006**, *45*, 8672−8676.

(19) (a) Xue, D.-X.; Cairns, A. J.; Belmabkhout, Y.; Wojtas, L.; Liu, Y.; Alkordi, M. H.; Eddaoudi, M. *J. Am. Chem. Soc.* **2013**, *135*, 7660−7667. (b) Lin, R.-B.; Chen, D.; Lin, Y.-Y.; Zhang, J.-P.; Chen, X.-M. *Inorg. Chem.* **2012**, *51*, 9950−9955.

(20) Myers, A. L.; Prausnitz, J. M. *AIChE J.* **1965**, *11*, 121−127.

(21) (a) Nugent, P. S.; Rhodus, V. L.; Pham, T.; Forrest, K.; Wojtas, L.; Space, B.; Zaworotko, M. J. *J. Am. Chem. Soc.* **2013**, *135*, 10950−10953. (b) Tan, Y.-X.; He, Y.-P.; Zhang, J. *Inorg. Chem.* **2012**, *51*, 9649−9654. (c) Li, B.; Wang, H.; Chen, B. *Chem. - Asian J.* **2014**, *9*, 1474−1498. (d) Xuan, Z.-H.; Zhang, D.-S.; Chang, Z.; Hu, T.-L.; Bu, X.-H. *Inorg. Chem.* **2014**, *53*, 8985−8990. (e) Li, J.-R.; Sculley, J.; Zhou, H.-C. *Chem. Rev.* **2012**, *112*, 869−932. (f) Xiang, S.; He, Y.; Zhang, Z.; Wu, H.; Zhou, W.; Krishna, R.; Chen, B. *Nat. Commun.* **2012**, *3*, 954.

(22) Park, H. J.; Suh, M. P. *Chem. Sci.* **2013**, *4*, 685−690.

(23) Demessence, A.; D'Alessandro, D. M.; Foo, M. L.; Long, J. R. *J. Am. Chem. Soc.* **2009**, *131*, 8784−8786.

DOI: 10.1021/acs.inorgchem.5b00987
Inorg. Chem. 2015, 54, 8937−8942

(24) Zheng, B.; Bai, J.; Duan, J.; Wojtas, L.; Zaworotko, M. J. *J. Am. Chem. Soc.* **2011**, *133*, 748−751.

DOI: 10.1021/acs.inorgchem.5b00987
Inorg. Chem. 2015, 54, 8937−8942